

JCTC

Journal of Chemical Theory and Computation

Stability of Hydrocarbons of the Polyhedrane Family Containing Bridged CH Groups: A Case of Failure of the Colle–Salvetti Correlation Density Functionals

Grigory A. Shamov,^{*,†,‡} Georg Schreckenbach,[†] and Peter H. M. Budzelaar[†]

*University of Manitoba, Winnipeg MB, Canada, and Dutch Polymer Institute (DPI),
P.O. Box 513, 5600 MB Eindhoven, The Netherlands*

Received July 13, 2010

Abstract: DFT-computed energies of polyhedral hydrocarbons, such as dodecahedrane $C_{20}H_{20}$, its smaller analogs $C_{16}H_{16}$ and $C_{12}H_{12}$, and the larger $C_{24}H_{24}$, estimated in comparison with corresponding isomeric hydrocarbons, vary widely with the choice of the density functional. In particular, large discrepancies were observed with the functionals that are based on the B88 (as well as G96, B86) exchange and the LYP (as well as OP) correlation parts. The problem is not related to the presence of the smaller cyclopropane rings in the $C_{12}H_{12}$ polyhedrane, for its hydrogenated products do show similar errors; moreover, the larger dodecahedrane that is free from the Bayer strain shows a similar trend. DFT-D corrections that are very useful in fixing long- and medium-range correlation issues with GGA DFT do not help in this case either. We show that these errors stem from the B88 (G96, B86) exchange functionals and are not compensated by Colle–Salvetti-based GGA correlation functionals such as LYP, OP, TCA, etc. However, they can be corrected by the PBE correlation functional based on the PW92 uniform electron gas (UEG) parametrization. Range-separated hybrids (likura and Hirao's LC-BOP, LC-BLYP) perform much better than the parent GGAs. Comparisons of polyhedranes with a well-studied system of similar size, the set of C_nH_n cyclophanes, reveal a completely different performance for the latter—for instance, RHF results are the poorest, and LC-type functionals do not give any improvement, but dispersion-corrected BLYP-D performs very well. We conclude that, while for polyhedranes medium-range delocalization errors from exchange dominate, for cyclophanes, the correlation/overlap-dispersion interactions are more important. The OPTX exchange functional shows significantly lower errors compared to B88 and G96; its combinations like OLYP and especially KT3 perform well for both test sets. The OPTX-based double hybrid, O2PLYP, also outperforms the corresponding B88-based B2PLYP functional for polyhedranes. Our computations also suggest that the $(CH)_{16}$ and $(CH)_{24}$ polyhedranes could be possible synthetic targets.

Introduction

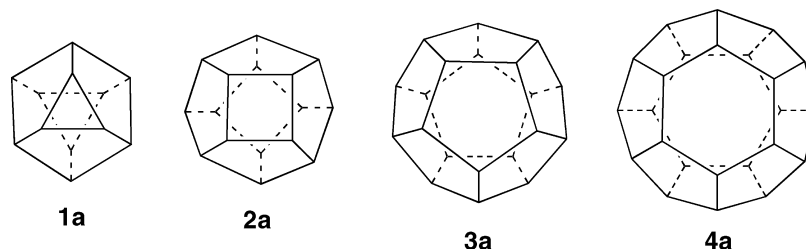
Cage and highly symmetric hydrocarbons are interesting due to their aesthetic appeal. The polycyclic caged hydrocarbons and their derivatives were very instrumental in developing the concepts of the theory of reaction mechanisms in organic

chemistry (see, for example, ref 1). The cage hydrocarbons **1a–4a** that we will discuss in this work (Scheme 1) are built from two parallel, staggered carbocycles linked into a three-dimensional cage by a rim of methyne bridges, so that a “tire” of fused five-membered rings is formed. The dodecahedrane **3a** (two cyclopentane rings) has been known for quite a while and was subject to numerous experimental and theoretical studies.^{2–6} The related compound **1a** was also recently synthesized and studied both experimentally and

* Corresponding author e-mail: gas5x@yahoo.com.

[†] University of Manitoba.

[‡] DPI.

Scheme 1. Polyhedranes $(\text{CH})_n$, for $n = 12, 16, 20$, and 24 

theoretically.⁷ Besides their geometrical beauty, there could also be potential applications, for example, for perfluorinated dodecahedrane⁸ which consists of two charged, nearly spherical layers, or using polyhedrane cages to encase atoms and small metal ions for some molecular electronic devices.^{9–11}

There is mounting evidence that the description of inter- and intramolecular interactions in large hydrocarbon systems can be problematic for density functional theory (DFT) methods, which are today the most widely used tools in theoretical organic and organometallic chemistry.^{12–19} This presents a challenge, since for realistic modeling of systems of chemical interest (for example, transformation of hydrocarbons catalyzed by a transition metal complex whose ligands are also hydrocarbons, or an enzyme reaction center, surrounded by several amino acid residues) it is important to have a balanced, reasonably correct description of all parts of the system under study. It would not do if only reaction barriers were correctly described, but not intra- and intermolecular interactions between reactants, ligands, and the surroundings, or vice versa.

Recent developments in the theory have shown that the reason for many problems of approximate DFT lies in its deficiency in the description of dispersion interactions.^{20,21} Also, most of the popular GGA and hybrid density functionals are over-repulsive at medium and large interatomic distances. Various methods were introduced to amend these DFT problems—among the most popular and computationally inexpensive are the CR^{-6} corrections by Grimme,^{22,23} named DFT-D, and the pseudopotential modification by the group of Röthlisberger,²⁴ adapted for Gaussian-basis molecular calculations by DiLabio et al.^{25,26} (C-Pot). It was thought¹³ that, while important, dispersion corrections alone cannot be sufficient to accurately describe intramolecular interactions in hydrocarbons and thus their relative stabilities with DFT. However, recent work in the area seems to show^{27,28} that, with the proper parametrization, DFT-D can in most cases successfully describe both intra- and intermolecular interactions in hydrocarbons by correcting the over-repulsive nature of GGA and hybrid functionals at medium-range interatomic distances. This leads to the question of whether the correction can still be called “dispersion”, or whether it is some other exchange-correlation error that is being corrected, perhaps the delocalization error described by Yang and co-workers.¹² The C-Pot method also performs well for some functionals of a repulsive nature, like the popular B3LYP.²⁷ Very recently, a new revision of the DFT-D method, termed DFT-D3, was introduced; this revision tries to restrict the

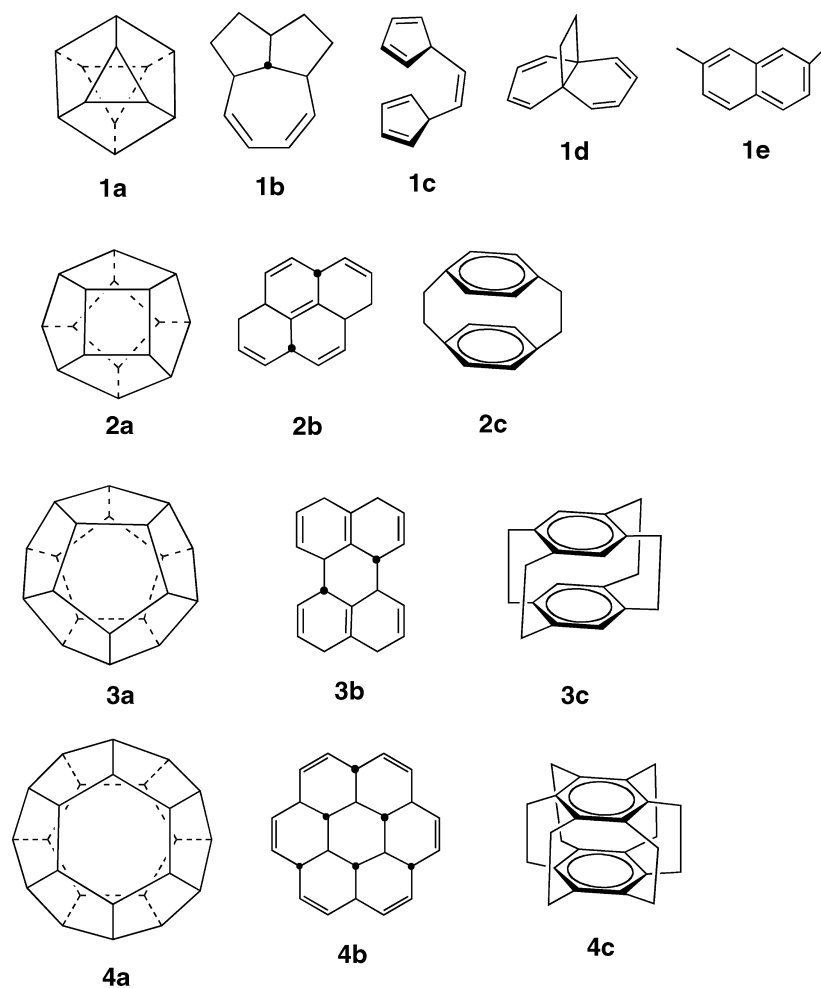
correction to the van der Waals interactions only, without correcting the medium range behavior of the GGA functionals.²⁹

In the recent work of Gill and co-workers,¹⁸ the problems of DFT with reactions that lead to an increased degree of hydrocarbon branching were attributed mainly to errors in the DF exchange functionals (i.e., not to the Coulomb or the kinetic energy, or a correlation functional).

A particularly interesting case however exists where some DFs fail only for some of the combinations of exchange and correlation functionals. It was found previously¹⁴ that for the $(\text{CH})_{12}$ compound **1a** (Scheme 1), named [D_{3d}]-octahedrane by its creators, the performance of density functionals varies widely; the authors issued a cautionary warning for using DFT for “structures with single bonds only, especially for small rings”. Earlier, we showed²⁷ that for the $(\text{CH})_{12}$ isomers, some combinations of exchange and correlation functionals, most notably the combination of Becke’s popular B88 exchange³⁰ with the LYP^{31,32} correlation, show large discrepancies from results using other functionals and the MP2 method. Numbers provided in the paper by Schreiner and co-workers¹⁴ also show that some other functional combinations, for example, Gill’s GLYP³³ functional, behave similarly to BLYP. Not all density functionals perform similar to BLYP–PBE, for example, yield results much closer to those by correlated wave function methods. We have shown that the OLYP functional, which is strongly over-repulsive at medium range, describes the stability of the [D_{3d}]-octahedrane well; moreover, the BPBE combination also performs well. DFT-D was found to be insufficient to amend the performance of the combination of Becke’s B88 and LYP (but the C-Pot method with B3LYP has, rather unexpectedly, been successful).

Thus, it is interesting to investigate why a specific combination of exchange and correlation functionals suddenly performs poorly for this specific hydrocarbon case. As was alluded to above, it is always desirable for a density functional to provide a balanced description of the model systems under study. Information on which functional is successful for which kind of system can be essential for possible practical applications. We dedicate this article to answering these two questions for the curious case of octahedrane and related compounds.

To do that, we have applied a systematically chosen set of density functionals, in some cases together with methods that include dispersion interactions (DFT-D by Grimme²³ and C-Pot by DiLabio and Mackie²⁵) in the computation of the stabilities of $(\text{CH})_n$ cage molecules ($n = 12, 16, 20, 24$),

Scheme 2. Isomeric C_nH_n Molecules, $n = 12, 16, 20$, and 24 , Used to Estimate the Stabilities of **1–4**^a

^a Tertiary carbons of the condensed polycycles **1b–4b** for which hydrogens point up are labeled with black dots; otherwise the hydrogens point down.

shown in Scheme 1. For comparison, we will use isomeric cyclophanes (Scheme 2) that contain stacked π -rings at close distances. For the cyclophanes, the importance of the intramolecular dispersion interactions is well established; these molecules have been thoroughly studied theoretically.^{34–36}

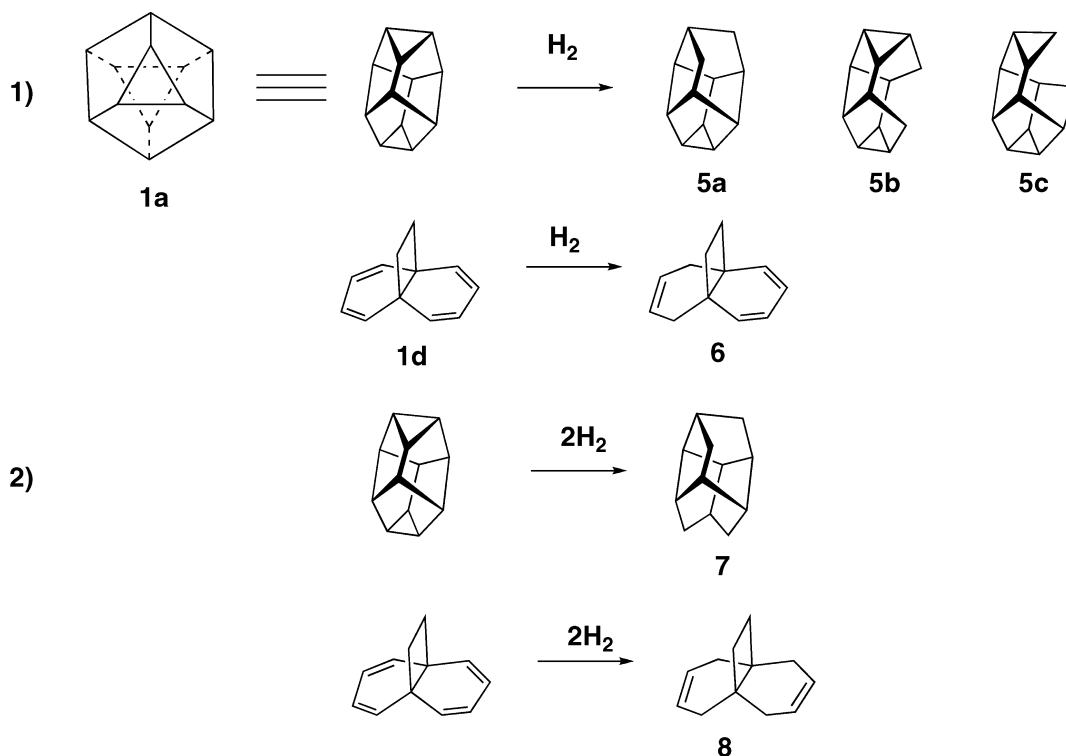
The presence of small carbocycles and sterical strain are the popular culprits when DFT methods happen to fail for molecules like the compound **1a**, $(CH)_{12}$. In the present work, we extend the range of polyhedranes from the highly strained compound **1a**, which contains cyclopropane rings, to the larger polyhedrane cages **2a–4a**. The set includes dodecahedrane **3a**, which is a compound with angles around its carbons close to tetrahedral, and thus free from the Bayer (angular) strain. (We note that in **3a**, as well as in all of the polyhedranes under study, another type of steric strain³⁷ is present, due to the eclipsed conformation of carbon–carbon dihedrals; for dodecahedrane, its value was estimated in refs 4 and 38.) We will investigate whether for these compounds a similar picture of the performance of density functionals will be observed.

Following the current trend³⁹ of DFT benchmarking studies, as a measure of stability, we will consider relative energies of isomeric hydrocarbons rather than heats of their

formations or atomizations, thus avoiding complications with the treatment of open-shell atoms. In addition, in order to assess the stabilities of the $(CH)_n$ cage compounds relative to each other, we will consider their formation energies from acetylene C_2H_2 .

We have selected isomers of C_nH_n , to act as references for evaluating the stabilities of polyhedranes in the following way. First, the isomers must be nonpathological cases for DFT. For instance, they should not have extended conjugated systems, which excludes annulene $(CH)_n$ systems. Second, they should be of approximately the same type of compound for the entire range of n values in the C_nH_n family, to allow for more or less justified comparisons between the stabilities of the different polyhedranes.

On the basis of these criteria, we have constructed several isomers of C_nH_n , borrowing some from our previous work,²⁷ and some from ref 14. The structures are presented in Scheme 2. For $(CH)_{24}$, the partially hydrogenated coronene **4b** was chosen, for it is planar (i.e., has minimal nonbonded C–C contacts), made of six-membered rings only, and yet is a nonconjugated hydrocarbon. Similar types of hydrocarbons for $C_{20}H_{20}$ and $C_{16}H_{16}$, structures **3b** and **2b**, correspondingly, were chosen. (They are not precisely of $(CH)_n$ type, but this

Scheme 3. Hydrogenation Products of the Polyhedrane **1a** and Tricyclohexatetraene **1b**

is not important for our purposes). For $C_{12}H_{12}$, we chose compound **1b** (which is compound **21** from ref 14; note that it is not the most stable, but the most symmetrical one of its isomers). In addition, structures of the tricyclo-dodecatetraene **1d** and 2,7-dimethylnaphtalene **1e** were considered isomers of $C_{12}H_{12}$.

For our second set of compounds, we chose the paracyclophanes **2c**, **3c**, and **4c** as isomers for C_nH_n for n greater than twelve. For the $C_{16}H_{16}$, meta-cyclophane **2d** was also computed. For $C_{12}H_{12}$, the selection of a real cyclophane is impossible; for that reason, we picked the molecule **1c**, *cis*-(bis-cyclopentadienyl)ethylene, in which the unsaturated five-membered rings are roughly parallel. Note that along the series **1c–2c–3c–4c**, the steric strain increases, and the unsaturated/aromatic rings get closer to each other.

In the original paper dedicated to $[D_{3d}]$ -octahedrane **1a** by Schreiner et al.,⁷ the mono- and dihydrogenated species **5a–c** and **7** (Scheme 3) were also considered; we will include them along with the tricyclododecatetri- and -dienes **6** and **8**, correspondingly, of which the former are isomers.

In this work, we will investigate the performance of various combinations of exchange and correlation functionals. First, we will apply the BLYP and GLYP functionals that perform poorly, and the OLYP, PBE, and BPBE functionals that perform well for $[D_{3d}]$ -octahedrane,²⁷ to the wider set of test compounds (Schemes 1–3). Second, we will systematically test the density functionals, by using stand-alone exchange, as well as mixing and matching exchange and correlation functionals of various kinds; to apply modifications such as the inclusion of a fraction of the Hartree–Fock exchange, both global and range separated (LC-corrections by Iikura et al.^{40,41}), as well as double hybrids, which in addition to a high fraction of exact exchange contain a portion of the PT2 correlation energy.⁴²

The generalized gradient approximation for exchange–correlation energy is written as follows:

$$E_{XC} = \sum_{\sigma} E_{X\sigma} + E_C \quad (1)$$

$$E_{X\sigma} = \int e_{LDA,\sigma}(\rho_{\sigma}) F(x_{\sigma}) d^3r; x = |\nabla\rho|/\rho^{4/3} \quad (2)$$

Here, F , which depends on the reduced density gradient x , is the GGA enhancement factor, introduced to improve the performance of the local density approximation for systems that differ from the uniform electron gas (UEG; its energy being determined by $e_{LDA}(\rho)$), such as atoms and molecules. Further, $\sigma = \alpha$ and β denotes the spin component. We provide plots of the enhancement factors $F(x)$ for selected functionals in the Supporting Information (Figure S2).

The correlation energy E_C , unlike the exchange energy, depends on both spin densities. Sometimes it can be written with same-spin and opposite-spin correlation contributions separated.

$$E_C = E_{C,\alpha\beta}(\rho_{\alpha}, \rho_{\beta}, x_{\alpha}, x_{\beta}) + \sum_{\sigma} E_{C,\sigma\sigma}(\rho_{\sigma}, x_{\sigma}) \quad (3)$$

The forms of its dependency on the spin densities and their gradients that are used in the literature vary. One of the approaches is to use an approach similar to the exchange functional: take a local correlation energy functional and add gradient corrections to it. There is no analytical solution for the uniform electron gas correlation energy, unlike for the exchange part where such a solution is known. Parameterized forms, interpolating numerical results exist; the most popular are the VWN⁴³ and PW92⁴⁴ functionals, although recently others were proposed also.⁴⁵ Besides GGA-corrected UEG-based correlation functionals

such as PBE, meta-GGA correlation functionals such as VS98⁴⁶ and its modifications, the M06 family of functionals,⁴⁷ as well as many others exist.

Another approach to the DFT correlation energy is to derive a correlation functional *ab initio*, via a series of simplifications—for example, starting from the Colle–Salvetti formula derived from a correlated wave function for the helium atom using a series of approximations. An example is the popular LYP³¹ functional in the form derived by Miehllich et al.³² The older Wigner⁴⁸ formula can be seen as the local part of LYP. Recently, several other Colle–Salvetti type functionals were proposed, most notably the OP by Tsuneda et al.,⁴⁹ Handy and Cohen’s CS1⁵⁰ functional, and the RC local functional⁵¹ and its GGA development called TCA.⁵² Other GGA correlation functionals building on the Wigner formula, such as the Wilson–Levy functional, have been proposed; see the recent work of Thakkar and McCarthy for their extensive evaluation.⁵³

Most of the energy contribution comes from the exchange functional. Thus, its asymptotic behavior is considered the most important. Dynamic correlation is also more short-range; however, nondynamic, or “left–right” correlation energy, is delocalized. It is well established that the inclusion of some fraction of the Hartree–Fock exchange⁵⁴ improves the performance of GGA functionals in many cases, such as the prediction of thermochemistry and reaction barriers. Recently, range separated forms of hybrid density functionals were proposed^{55–58} for which the amount of HF exchange is not constant but varies—for example, from GGA at short distances to HF for long distances. The long-range corrected GGAs show improved performance for properties that depend on the asymptotic behavior of the exchange, which is incorrect for GGA but can be reproduced by HF; at the same time, the electron–electron cusp condition, which is short ranged, is better described by DFT.

Recent attempts were made to include a fraction of the MP2 correlation energy computed with DFT orbitals, leading to the so-called double hybrids.⁴² Below, we will attempt to arrange the functionals to be tested in this work into groups.

Exchange Functionals

Group A. B88 and G96 are repulsive functionals; they are also the ones that perform poorly with the LYP correlation for octahedrane. These functionals exhibit a diverging $F(x)$ for the high limit of the reduced density gradient x . They are purely repulsive at any range of the PES. (See the scans in the Supporting Information, Figure S1.)^{59,60}

We have also included the B86 functional (with the formula taken from the Appendix of ref 59), which is similar to B88 but has a different “asymptotic behavior”, that is, a converging $F(x)$, which results in it showing some attraction at large interatomic distances. We note that for medium and short distances, B86 is over-repulsive, which is typical for all GGAs. (See the potential energy surface scans in the Supporting Information, Figure S1.) We also included the OPTX exchange functional, which has a higher power of x than B86 and violates the UEG limit. It is known^{27,61} that

OPTX is too repulsive at medium and short interatomic distances, even more so than B88. However, for long distances, it shows some attraction, just like B86. This can be traced to the shape of the $F(x)$ enhancement factor.⁶⁰

We will use the B88, G96, and OPTX exchange functionals in a stand-alone manner, naming them HFB, HFG, and HFO, and will match them with a variety of correlation functionals, as described below. We will also augment them with a fraction of HF exchange, globally (B3LYP) and in the long-range only (LC functionals for a few of the combinations). Moreover, we will try global double hybrids that include the PT2 correlation for some of them, namely, B2PLYP and our O2PLYP.

The power series B97 family functionals⁶² are also built on the basis of sums of B86-like expressions up to the second or fourth power. This is combined with a “spin-scaled” UEG PW92 correlation functional with GGA-corrections of a form similar to the B86 exchange. We have included in our set of functionals the original B97 hybrid functional and Grimme’s B97-D²³ GGA functional that has been optimized together with the dispersion correction, to avoid double counting of the long-range attractive interactions.

Recently, Goerigk and Grimme performed a reparameterization of commonly used density functionals, including BLYP, on the basis of their extensive benchmark database GMNKT,⁶³ again with inclusion of the DFT-D corrections. The latter was used in its reparameterized form, with the scaling factor for the R_0 radii increased to 1.34 from 1.1 and a global scaling factor of 1.0, giving it the correct asymptotic behavior at very long range. We include the reoptimized B88 + LYP combination, named oBLYP-D, in our set of functionals.

An interesting modification to the OLYP functional exists in the literature⁶⁴—a same-spin correlation term by Keal and Tozer was added to the OLYP functional, which was reparameterized and called KT3. The local version containing the same term (KT1) was shown to perform well for π – π stacking.⁶¹ We have included the KT3 functional in our set of functionals.

Group B. Group B consists of functionals that are spuriously attractive at the long range and less repulsive in the medium range than those in group A. The most prominent example is the PBE exchange functional. It was proposed⁶⁵ to reparameterize it (as well as the parameters of the PBE correlation counterpart, correspondingly), to give a better description of solids. The modification, named PBEsol, became more attractive than PBE in the medium–long range, which was shown to improve its performance for hydrocarbons, namely, cyclophanes and octahedrane **1a**.⁶⁶ Recently, a further modification of PBEsol including the higher-power x term in the denominator was proposed⁶⁷ under the name regularized gradient expansion (RGE2). In our study, we will include the PBE, PBEsol, and RGE2 functional combinations.

The highly parametrized Minnesota density functionals that are based on the VS98 meta-GGA exchange-correlational functional also claim improved performance for the interactions of interest to this work. We have shown²⁷ previously that the M06-L functional is on the softer side, performing comparably to PBE-D. We will include the local M06-L

Table 1. Combinations of Exchange and Correlation Functionals Employed in This Work

correlation functional		“repulsive” GGA	“softer” GGA and meta-GGA	large amount of exact exchange (hybrids/double hybrids)
none		HFB, HFG, HFO		RHF
LDA	UEG ^a	BPW92		
	CS ^b	BW		
GGA	UEG ^a	BPBE, BPBE-D, OPBE, B97, B97-D	PBE, PBEsol, RGE2, M06-L	M06-2X
	CS ^b	BLYP, BLYP-D, B3LYP, B86LYP, GLYP, BOP, oBLYP-D, OLYP, OLYP-D, O3LYP, KT3, B3LYP, B3LYP-C	TCA	B2PLYP, O2PLYP, BLYP-LC, BOP-LC, GLYP-LC

^a Correlation functionals based on a Uniform Electron Gas parametrization. ^b Correlation functionals based on the Colle–Salvetti formula.

functional and the hybrid that has been recommended by the authors for hydrocarbons, M06-2X, for comparison with the GGAs under study.

Correlation Functionals

Earlier, we showed²⁷ that, for [D_{3d}]-octahedrane, the BLYP combination of LYP with B88 did not work well, while BPBE did. In this paper, we will try to explain this observation and test this and related combinations on similar chemical systems (Schemes 1–3).

LYP is a GGA Colle–Salvetti⁶⁸ functional, while PBE correlation is a GGA based on the PW92 parametrization of the uniform electron gas (UEG). We will try to match the B88 exchange with LYP and PBE correlations; we will also try the B86LYP, OLYP, and OPBE combinations. Besides that, another Colle–Salvetti GGA functional, the one-parameter progressive (OP) functional by Tsuneda and co-workers,⁴⁹ will be combined with B88 and G96, giving the BOP and GOP functionals. Another recently introduced Colle–Salvetti functional, TCA, will be used, as proposed by its authors,⁶⁹ together with the PBE exchange.

To extend our study further, we will use LDA correlation functionals that correspond to the UEG parametrization (PW92) and to the Colle–Salvetti type. For the latter, we will try the Wigner functional, which can be roughly considered as an LDA part of the GGA LYP.^{50,70}

Combinations

Exchange-correlation functional combinations considered in this work are summarized in Table 1. Following our earlier work, to illustrate the “repulsiveness” of these functionals at medium and long interatomic distances, we have performed a PES scan of colliding the methane molecule into the ethane molecule, decreasing the intermolecular carbon–carbon distance from 6.0 to 2.0 Å. The interaction curves and details of the computations are provided in the Supporting Information (Figure S1).

Computational Methods

Geometry optimizations for the BLYP, BPBE, OLYP,⁷¹ and PBE⁷² density functionals were done using the Priroda code^{73–75} in the L11⁷⁴ basis set (a cc-pCVDZ-quality general contracted basis). The RI-JK approximation as implemented in Priroda⁷³ was applied throughout, with corresponding optimized density fitting basis sets. For GGA functionals, analytical second derivatives were computed on the opti-

mized geometries to confirm the nature of the respective minima. Final GGA energies were calculated on the L11 optimized geometries with the L22 basis set⁷⁴ (a cc-CVTZ-quality general contracted basis). RI-MP2 geometry optimizations were done with Priroda as well, in the cc-pVTZ-quality L2 basis.⁷⁴

To extend our study to a broader and more systematic range of functionals, and in particular to include various exchange-correlation functional combinations not available in Priroda, we have used a locally modified version of the MOLCAS code, version 7.4.^{76,77} For some functionals available in the regular version of MOLCAS, parameters were changed so that the optimized version of the BLYP functional by Goerigk and Grimme (oBLYP-D)⁶³ and PBEsol⁶⁵ were also implemented. The exchange functionals G96,³³ B86 (with the formula and parameter values taken from the Appendix of ref 59), OPTX⁷¹ and KT3,⁶⁴ and RGE2⁶⁷ (paired with the PBEsol exchange), as well as the correlation functionals by Wigner^{48,78} and the TCA⁵² correlation functional, were added to the code. On the basis of these additions, the following combinations were tested as single-point calculations on RI-MP2/L2 geometries in the same L22 basis set as for the Priroda computations: (1) pure exchange, with no correlation part—HFB, HFG, HFO—and (2) various GGA functionals named in the text as BLYP/MP2, B86LYP, GLYP, BPBE, BW,⁴⁸ BPW92 (with the local correlation functional of Perdew and Wang⁴⁴), OPBE, KT3, the hybrid functionals B3LYP⁵⁴ and O3LYP,^{71,79} the double-hybrid functional B2PLYP of Grimme,⁴² and its double hybrid analog that we will call O2PLYP using OLYP as the starting point. For the O2PLYP functional, we did not optimize the contributions from the exact exchange and the PT2 correlation but instead took the “physically motivated” values of 50% and 25%, correspondingly. For the GGA part of the O2PLYP exchange, we also took 50% of the original OPTX parameters for its LDA and GGA parts. For both of the double hybrids, in Tables 2–4, we provide energies due to the DFT part only, labeled B2PLYP(0), and with inclusion of the PT2 term (B2PLYP(2), correspondingly, except for Figures 1 and 2, where the functional is simply labeled B2PLYP).

We have also computed canonical MP2 and scaled opposite spin MP2 (SOS-MP2)⁸⁰ energies with the same L22 basis set using MOLCAS. All MOLCAS calculations, both DFT and MP2, were done using the compact atomic Cholesky decomposition technique (acCD) with an accuracy threshold of 1×10^{-4} .^{81–83}

Table 2. Binding Enthalpies Per Acetylene Monomer ΔE_b^b of Polyhedranes **1a–4a**, kcal/mol^a

method	1a	2a	3a	4a	MAD
SOS-MP2	<i>−44.2</i>	<i>−48.7</i>	<i>−53.0</i>	<i>−51.6</i>	
MP2	−4.4	−4.0	−4.2	−4.1	4.2
B2PLYP(0)	2.2	2.7	2.7	3.0	2.6
B2PLYP(2)	1.1	1.4	1.5	1.6	1.4
HFB	27.8	29.3	30.4	30.9	29.6
HFO	19.8	22.2	23.8	24.6	22.6
HFG	27.9	29.5	30.8	31.4	29.9
M06-L	−4.2	−2.7	−2.1	−1.9	2.7
M06-2X	−3.8	−2.9	−2.9	−2.8	3.1
KT3	−10.3	−10.2	−9.9	−9.7	10.0
B86LYP	10.3	11.0	11.4	11.6	11.1
BLYP ^c	9.2	9.8	10.3	10.5	9.9
BPBE-D ^c	5.3	4.7	4.8	4.6	4.8
BPBE ^c	−1.0	0.0	0.7	1.0	0.7
BPBE-D ^c	−4.4	−4.5	−4.2	−4.3	4.3
OLYP ^c	1.9	3.6	4.6	5.1	3.8
OLYP-D ^c	−1.9	−1.6	−1.0	−0.9	1.3
PBE ^c	−5.5	−4.9	−4.5	−4.3	4.8
PBE-D ^c	−7.9	−8.1	−7.9	−8.1	8.0
BW	21.5	22.7	23.6	24.1	23.0
RHF	4.3	4.9	4.9	5.4	4.9
BLYP-LC ^d	−9.9	−8.6	−10.1	−10.0	9.6
GLYP-LC ^d	−10.7	−9.2	−10.9	−10.8	10.4
BOP-LC ^d	−7.6	−7.3	−7.2	−7.0	7.3
BOP ^d	11.6	12.6	13.3	13.7	12.8
B97 ^d	−2.1	−3.0	−1.8	−1.6	2.1
B97-D ^d	3.1	−1.0	3.1	2.9	2.5
O2PLYP(2)	−2.4	−1.7	−1.4	−1.1	1.6
O2PLYP(0)	−1.5	−0.6	−0.4	0.1	0.7
GLYP/MP2	9.6	10.4	11.0	11.3	10.6
oBLYP/MP2	6.5	7.0	7.3	7.5	7.1
oBLYP-D/MP2	2.8	3.3	3.2	3.1	3.1
BPW92	17.4	18.5	19.2	19.6	18.6
OPBE	−10.3	−8.7	−7.6	−7.0	8.4
PBEsol	−14.5	−14.3	−14.1	−14.0	14.2
B2PLYP-D	−1.4	−0.9	−1.1	−1.2	1.1
B3LYP-Cpot ^d	−10.7	−10.7	−12.1	−11.9	11.4
B3LYP	3.2	3.6	3.8	4.1	3.7
RGE2	−5.5	−4.9	−4.5	−4.4	4.8
O3LYP	−9.8	−9.1	−8.7	−8.5	9.0
TCA	9.6	11.4	12.2	12.6	11.4

^a The SOS-MP2 are actual values (*in italics*); for the other methods, differences with respect to SOS-MP2 values are shown.

^b $\Delta E_b = (E(C_2H_2)_m - mE(C_2H_2))/m$. ^c Priroda L22 energies on optimized geometries at the DFT/L11 level. ^d GAMESS-US cc-CVTZ energies on Priroda MP2/L2 geometries.

The MP2 method is the cheapest accurate correlated wave function method. It is well-known that for intramolecular interactions of hydrocarbons (see refs 27, 66, and 84 and references therein), the method errs systematically toward overbinding. It was also found that the various spin-scaled MP2 methods, such as SCS-MP2 and SOS-MP2, perform much better for hydrocarbons (although the description of other systems, such as hydrogen bound complexes, might deteriorate).⁸⁴ Specifically for the polyhedranes, SCS-MP2 was shown to give energies of isomerization of compound **1a**⁶⁶ closer to the CCSD(T) values than MP2. Our preliminary tests for the **1a** system have shown that SOS-MP2 energy differences are closer to CCSD(T) than the SCS-MP2 ones by about 2 kcal/mol. Thus, we used the SOS-MP2 energies computed with the MOLCAS code as the reference energies throughout this paper.

The DFT-D corrections for the dispersion energy for the GGA functionals BLYP, OLYP, BPBE, and PBE were done

Table 3. Relative Energies of Hydrogenated Species of **1a**, **5a–c**, and **7** with Respect to Tricyclododecatetraene **1b** and Its Hydrogenated Derivatives **6** and **8**, Correspondingly, kcal/mol^a

method	5a → 6	5b → 6	5c → 6	7 → 8	MAD
SOS-MP2	<i>35.0</i>	<i>9.9</i>	<i>−5.4</i>	<i>46.7</i>	
MP2	4.3	4.5	3.4	3.1	3.9
B2PLYP(0)	−13.9	−8.7	−13.5	−11.0	11.8
B2PLYP(2)	−10.8	−6.7	−9.8	−8.5	8.9
HFB	−46.7	−35.0	−39.1	−37.6	39.6
HFO	−27.7	−17.7	−21.2	−25.0	22.9
HFG	−43.2	−32.3	−36.2	−34.9	36.6
M06-L	−5.4	3.6	0.8	−9.7	4.8
M06-2X	−4.5	2.8	−0.8	−7.6	3.9
KT3	1.4	4.9	2.5	0.2	2.2
B86LYP	−30.5	−21.2	−25.1	−24.6	25.4
BLYP ^b	−27.4	−37.9	−3.6	−22.5	22.9
BLYP-D ^b	−25.5	−35.7	−1.8	−20.7	20.9
BPBE ^b	−8.7	−20.2	13.1	−9.4	12.8
BPBE-D ^b	−7.1	−18.4	14.7	−8.0	12.1
OLYP ^b	−9.4	−20.7	12.8	−10.7	13.4
OLYP-D ^b	−7.6	−18.6	14.5	−9.0	12.4
PBE ^b	−6.3	−18.3	14.9	−7.3	11.7
PBE-D ^b	−5.3	−17.1	16.0	−6.4	11.2
BW	−39.8	−28.9	−33.2	−32.1	33.5
RHF	−12.5	−8.8	−14.6	−9.2	11.3
BLYP-LC ^c	1.7	5.1	1.9	−0.7	2.4
GLYP-LC ^c	2.9	6.0	2.8	0.3	3.0
BOP-LC ^c	2.1	5.8	2.6	−0.9	2.9
BOP ^c	−27.4	−18.5	−22.0	−22.5	22.6
B97 ^c	−9.6	−5.6	−8.8	−7.8	7.9
B97-D ^c	−21.2	−11.4	−15.2	−18.8	16.6
O2PLYP(2)	−1.8	1.6	−1.2	−2.6	1.8
O2PLYP(0)	−4.5	0.0	−4.4	−4.9	3.5
GLYP/MP2	−23.9	−16.2	−19.7	−19.3	19.8
oBLYP/MP2	−24.3	−16.4	−19.9	−19.7	20.1
oBLYP-D/MP2	−27.3	−16.1	−19.0	−23.0	21.3
BPW92	−35.4	−25.1	−29.4	−28.6	29.6
OPBE	12.8	16.4	14.6	6.0	12.4
PBEsol	5.8	9.2	7.3	2.3	6.2
B2PLYP-D	−12.4	−6.1	−9.0	−10.3	9.4
B3LYP-Cpot ^c	0.9	1.6	−1.4	1.2	1.2
B3LYP	−17.8	−11.1	−15.2	−14.6	14.7
RGE2	−5.9	−0.1	−2.7	−6.8	3.9
O3LYP	2.4	6.7	3.7	−0.3	3.3
TCA	−23.4	−12.6	−16.2	−21.9	18.5

^a The SOS-MP2's are actual values (*in italics*), while for other methods, differences with respect to it are shown. ^b Priroda L22 energies on optimized geometries at the DFT/L11 level. ^c GAMESS-US cc-CVTZ energies on Priroda MP2/L2 geometries.

according to Grimme's 2006 formulation,²³ using the BOptimize code⁸⁵ with the scaling factors being the same as in our previous work,²⁷ as single-point energy computations on the GGA optimized geometries. For the B2PLYP-D and oBLYP-D functionals, dispersion corrections were also computed with BOptimize, using the recommended scaling factors. We have also tried to optimize geometries with GGA DFT-D for some cases, such as the para-cyclophanes **2c** and **3c**. While the geometry changes were not negligible, the relative energy changes were. Hence, we use single-point energies throughout.

In addition, we have investigated the one-parameter progressive correlation functional (OP) by Tsuneda et al.⁴⁹ together with the B88 exchange functional (BOP), Grimme's²³ pure power series GGA optimized with dispersion correction (B97-D), and the original power series hybrid functional B97 by Becke.⁶² Also, the performance of the

Table 4. Calculated Relative Energies of Isomers of Compounds 1–4, kcal/mol^a

method	1a → 1e	1a → 1d	1b → 1a	1b → 1c	2b → 2a	2b → 2c	3b → 3a	3b → 3c	4b → 4a	4b → 4c
SOS-MP2	-34.8	24.6	-35.2	5.4	-56.0	-44.4	-85.4	-41.3	-70.2	-35.7
MP2	-7.3	5.5	-6.4	-0.5	-3.8	-11.0	-3.7	-8.5	-5.0	-9.3
B2PLYP(0)	-32.1	-13.9	13.2	-2.2	22.3	4.1	29.0	28.2	21.7	42.2
B2PLYP(2)	-27.3	-11.2	10.4	-2.5	17.1	-2.9	22.3	12.3	15.7	17.6
HFB	-77.5	-51.9	49.4	-15.4	68.6	-5.8	88.4	30.9	73.2	45.1
HFO	-49.9	-26.8	26.1	-11.7	41.2	1.0	58.0	36.0	42.3	53.2
HFG	-73.4	-47.8	45.7	-14.4	63.6	-3.8	82.9	32.4	67.3	45.5
M06-L	-17.5	-0.5	-0.5	-3.2	11.9	-7.7	24.2	6.0	16.6	5.2
M06-2X	-10.7	-0.3	-0.5	-1.8	10.6	-0.3	15.6	11.6	12.1	19.6
KT3	-9.4	4.6	-3.3	2.3	-5.4	1.8	-4.1	13.8	-14.6	16.0
B86LYP	-54.4	-33.1	31.5	-8.5	43.9	-5.2	56.3	20.3	43.7	28.6
BLYP ^b	-49.4	-30.1	28.0	-9.1	39.9	-4.1	51.1	18.8	39.0	26.7
BLYP-D ^b	-41.7	-28.4	25.3	-5.4	28.6	-10.0	37.2	0.5	30.4	3.6
BPBE ^b	-21.6	-6.1	6.4	-4.6	13.6	1.1	21.1	17.8	9.8	22.8
BPBE-D ^b	-14.9	-4.9	4.1	-1.0	3.7	-4.3	8.7	1.5	2.1	2.6
OLYP ^b	-23.7	-6.1	6.4	-7.3	15.9	2.3	25.5	24.6	13.5	36.8
OLYP-D ^b	-16.1	-4.7	3.9	-2.7	4.3	-3.6	11.0	6.0	4.3	13.7
PBE ^b	-17.9	-3.6	4.1	-2.5	9.8	0.4	15.6	13.9	5.6	17.1
PBE-D ^b	-13.1	-2.8	2.5	-0.5	2.7	-3.7	6.7	2.1	0.0	2.8
BW	-68.5	-43.9	41.5	-12.8	58.0	-5.2	74.8	28.1	59.5	39.6
RHF	-27.8	-12.7	11.9	-0.9	22.2	13.3	29.2	43.2	25.2	66.9
BLYP-LC ^c	-1.5	6.1	-5.4	2.4	8.6	8.6	-0.9	18.6	-4.7	25.4
GLYP-LC ^c	0.1	7.5	-6.6	2.8	8.9	9.0	-3.2	18.5	-6.9	25.2
BOP-LC ^c	-1.0	7.2	-6.4	1.5	-1.9	9.8	-0.7	22.0	-5.9	29.7
BOP ^c	-50.1	-29.0	27.7	-8.6	39.9	-2.6	52.2	23.9	38.1	31.6
B97 ^c	-24.2	-8.8	8.7	-2.1	3.5	2.0	15.8	20.4	5.3	27.6
B97-D ^c	-35.1	-21.6	19.2	-5.7	-8.6	-10.5	30.9	1.0	24.1	6.5
O2PLYP(2)	-14.2	0.8	-0.6	-0.7	4.1	0.8	8.1	15.3	0.9	22.0
O2PLYP(0)	-18.2	-1.4	1.6	-0.4	8.5	7.2	13.6	30.0	5.8	44.9
GLYP/MP2	-46.6	-25.6	24.7	-6.4	35.0	-1.9	46.0	21.8	33.0	27.1
oBLYP/MP2	-46.1	-26.2	25.1	-6.0	35.3	-3.7	45.7	18.2	33.8	23.5
oBLYP-D/MP2	-34.8	-19.6	17.7	-6.0	26.6	-9.8	33.0	4.0	25.6	10.4
BPW92	-63.1	-38.7	36.4	-11.2	51.5	-4.9	66.4	26.3	51.2	36.4
OPBE	8.0	21.5	-18.7	2.4	-17.4	8.9	-13.8	23.1	-25.3	28.8
PBEsol	-0.9	10.6	-8.5	3.6	-7.6	3.0	-5.5	9.3	-13.3	7.3
B2PLYP-D	-19.6	-6.7	5.1	-1.8	11.9	-6.4	15.6	3.1	11.7	7.3
B3LYP-Cpot ^c	-6.7	2.5	-7.0	1.1	-3.0	-4.0	-14.2	-1.1	-16.6	-2.8
B3LYP	-37.7	-18.3	17.5	-4.0	26.8	-0.8	34.9	21.0	24.9	29.0
RGE2	-17.9	-3.0	3.7	-1.0	8.6	0.4	14.3	14.3	4.2	16.5
O3LYP	-8.2	7.1	-5.8	1.8	-2.0	4.0	1.5	17.7	-7.5	22.6
TCA	-42.4	-22.0	21.0	-8.4	36.6	-2.5	50.3	23.9	37.5	34.1

^a See Scheme 2 for a description of the isomers. The SOS-MP2 values are the actual isomerization energies (*in italics*); for the other methods, differences from the SOS-MP2 values are shown. ^b Priroda L22 energies on optimized geometries at the DFT/L11 level. ^c GAMESS-US cc-CVTZ energies on Priroda MP2/L2 geometries.

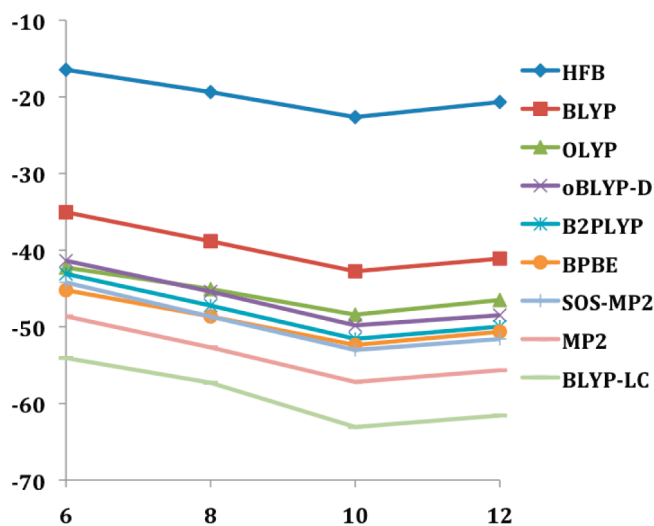


Figure 1. Binding energies of polyhedranes $(\text{CH})_{2n}$ from n molecules of acetylene, per acetylene monomer (eq 1), kcal/mol.

range-separated hybrid functionals by Hirao et al.⁴⁰ (long-range correction, LC) was studied for the BLYP-LC, BOP-LC, and GLYP-LC functionals. Finally, C-Pot computations were done with the B3LYP/cc-CVTZ basis, with C-Pot coefficients optimized for B3LYP/aug-cc-pVTZ taken from ref 25. We have used test calculations to ensure that the difference in the basis sets does not lead to significant changes in MAD values for the carbon-only subset of the S22 set; thus, the pseudopotential parameters are transferable enough. These computations were done with the GAMESS-US⁸⁶ code, version February 2009, using single point energy calculations in the cc-CVTZ basis by Dunning and Hay⁸⁷ on the Priroda RI-MP2/L2 optimized geometries.

Results and Discussion

Geometries of the Hydrocarbons. For the cage molecules 1a–4a and tricyclooctane 5, all GGA DFs for which we did optimize geometries show very similar bond angles. In the dodecahedrane 3a, the CCC angles are equal to 108°, while the CCH angles are 110.9°. Going from 1a to 2a and 4a,

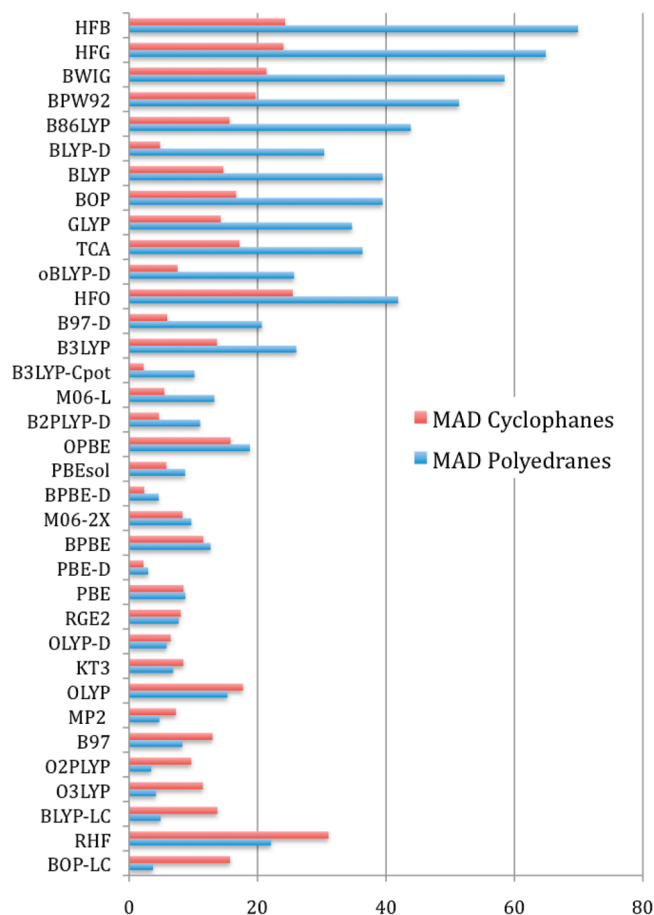


Figure 2. Mean absolute differences (MAD) for cyclophane and polyhedrane isomerization, relative to SOS-MP2 computed values, kcal/mol.

the $C_bC_bC_b$ angle (the angle between the bridge carbons) rises from 100.8° in **1** to 107.8° – 107.9° in **4**; the $C_bC_bC_3$ angle (the angle between two bridge and one top cycle carbon) increases from 106.2° – 106.3° to 108° . The angles including bridge hydrogens decrease from 113.7° to 111.3° in this series. All of these changes indicate that, for the larger polyhedranes, steric strain due to the angular deformation of bridged carbons decreases. The optimized bond lengths are also similar for all of the GGA DFs, except BLYP, which systematically yields longer C_b – C_3 and C_b – C_b bonds in **1a**–**4a**.

The geometries of **1a**–**4a** optimized at the RI-MP2/L2 level show $C_bC_bC_b$ and $C_bC_bC_3$ angles very similar to the DFT ones. Both C_b – C_3 and C_b – C_b bond lengths are usually shorter at the GGA DFT level, OLYP showing the closest agreement in bond length with RI-MP2. All of the geometries of compounds **1a**–**4a**, **1b**–**4b**, and **1c**–**4c** are provided in the Supporting Information as a separate file.

Binding Energies of 1a–4a Relative to Acetylene. The binding energies of the polyhedranes **1a**–**4a** relative to acetylene were weighted per acetylene monomer according to eq 4:

$$E_{\text{bind}} = (1/n) \times E(C_{2n}H_{2n}) - E(C_2H_2) \quad (4)$$

The calculated values are collected in the Table 2 as differences from the SOS-MP2 values. For selected methods, the absolute values are also pictured in Figure 1.

One can see that all methods predict an increase of binding from **1a** to **3a**, which is the most stable polyhedrane, with **4a** slightly less stable than **3a**. This is what one would expect on the basis of the angular strain argument—the angles around the carbon atoms in **4a** and especially **3a** are closest to tetrahedral. The absolute values of the binding energies vary strongly between the computational methods; however, within the series of the polyhedranes, each method performs similarly. That is, the presence of the small cyclopropane and cyclobutane rings in **1a** and **2a** and their absence in **3a** and **4a** does not lead to significant changes in the order of the energies calculated.

In Figure 1, it can be seen that BLYP underestimates the binding energy as compared to SOS-MP2. The exchange-only HFB yields unrealistically small binding. MP2 and BLYP-LC overbind, the latter quite strongly. OLYP, which is quite an over-repulsive functional, is much closer to SOS-MP2 than BLYP; the reoptimized version of the latter, including dispersion corrections, oBLYP-D, performs better. The BPBE combination and the double hybrid B2PLYP functional also perform well.

A more systematic overview, with all of the functionals included in Table 1, shows that, not surprisingly, stand-alone exchange functionals perform much worse than those combined with a correlation functional. HFB and HFG have similarly large differences from the SOS-MP2 values. They are followed by BW and HFO, which are also close to each other, and then comes the BPW92 combination. It is interesting to observe that the pure OPTX exchange functional has much smaller errors than either B88 or G96 and, also, that the Wigner correlation functional (which can roughly be seen as the local part of the LYP correlation functional) is less efficient than the local PW92 correlation that is based on a uniform electron gas (UEG) parametrization.

The RHF method predicts results quite close to those of SOS-MP2 (with MAD under 5 kcal/mol). Many of the GGA combinations, such as BLYP, B86LYP, GLYP, BOP, and OPBE, perform worse. Using the long-range HF hybrids BLYP-LC, BOP-LC, and GLYP-LC does not significantly improve the MADs from SOS-MP2 over the corresponding pure GGAs. However, the sign of the deviations changes—long-range hybrids show overbinding, while pure functionals underbind (see for example BLYP in Figure 1). PBEsol and KT3, as well as the dispersion-corrected PBE-D, also show overbinding, as does the canonical MP2 method. The smallest deviations from SOS-MP2 were obtained for double hybrids; “repulsive” GGAs with DFT-D corrections such as BPBE-D, OLYP-D, oBLYP-D, and B97-D; the hybrid B97 functional; and the M06-family functionals. We note that B88 exchange improves when paired with PBE instead of LYP correlation, while for OPTX exchange, the situation is opposite.

The performance of the exchange functionals of the PBE family, especially PBEsol, is poor compared to B88 and OPTX. In this model system, the result might depend on the accuracy of the description of acetylene by a given method; since acetylene is a small, highly symmetric molecule, one could expect poor performance for functionals that do not do well for atoms, which is the case with PBE.

Thus, below, we will investigate isomerization and hydrogenation reactions that involve large molecules only as another way to assess the stabilities of the polyhedranes. But first, we will look into the hydrogenation reactions for the sterically strained compound **1a**.

Energies of Hydrogenated Compound 1: C₁₂H₁₄ and C₁₂H₁₆. The hydrogenation of compound **1a** had been studied theoretically in the original experimental work, employing MP2 and B3LYP computations in a small basis set.⁷ The authors have considered isomers **5a–5c**; it was also shown that the second stage of the hydrogenation leads preferentially to compound **7**. Considering isomers where some or all of the cyclopropane rings are opened due to hydrogenation, we can test whether the large deviations of the B88 + LYP combination are due to the strain introduced by the small cycles. To assess the relative energies, we have compared them to an isomeric molecule, tricyclododecatetraene **1d** in different degrees of hydrogenation, and **6** and **8** (Scheme 3). We would like to avoid using the actual hydrogenation process for the comparison, preferring to compare isomers. Results are presented in Table 3. One can see that the trends observed in our work (as well as in earlier publications by other authors) for the relative energies of **1a** and its isomers hold for the hydrogenated species **5a–c** and **7** as well: The BLYP functional (as well as the very similar functionals B86LYP, GLYP, and BOP but not OLYP and BPBE) strongly underestimates the stabilities of the hydrogenated derivatives of **1a**. Even for compound **7**, which has no cyclopropane rings at all, there is a perceptible difference in the performance of the different density functionals. Interestingly, going from pure GGAs to the long-range hybrids BLYP-LC and GLYP-LC removes the error. The double-hybrid functional O2PLYP and the pure GGA KT3 perform best among the functionals without dispersion corrections. Overall, the trends in the MADs for different methods are close to those for the isomerizations of polyhedranes **1a–4a**, which are considered in the following section.

Isomerization Energies of Compounds 1–4. We have computed the relative energies of isomerization of our “base reference compounds” **1b–4b** into the two sets of corresponding structures: polyhedranes **1a–4a** and cyclophanes **1c–4c** (considering **1c** as similar to cyclophane). The isomerization energies for **1a** and **1b** were published previously.^{14,27,66} We note that isomer **1b** is not the most stable one studied by Csonka et al.⁶⁶ The cyclophanes C₁₆H₁₆ (**2c** and **2d**) were subjects of several theoretical studies⁸⁸ thanks to their epitomizing of aromatic π – π interactions.⁸⁹

The results for isomerization reactions by different methods are collected in Table 4. Our calculations display a very distinctive feature of the performance of our computational methods: the MADs for two sets (corresponding to the reactions of **1b–4b** to either **1a–4a** or **1c–4c**, respectively) pictured in Figure 2 show that methods performing well for the cyclophanes tend to do poorly for the polyhedranes, and vice versa!

Let us first consider the cyclophanes. In contrast to the results of the previous sections (**1a** and its hydrogenated species) as well as the polyhedranes discussed below, the worst method for the cyclophanes is RHF (Table 3; Figure

2), with a MAD of over 30 kcal/mol. This is followed by the exchange-only functionals, with HFO being marginally worse than HFB and HFG, which have MADs of about 24 kcal/mol. The B88 exchange combined with the local correlation functionals, Wigner and PW92, also has large errors of about 20 kcal/mol; the DFT parts of the double hybrids (labeled O2PLYP(0) and B2PLYP(0), without the PT2 term) perform about as poorly as the former, owing to the large fraction of RHF exchange and the smaller portion of GGA correlation they contain. Next, this is followed by all of the “repulsive” GGA combinations such as OLYP, BOP, BLYP, B86LYP, and GLYP. Interestingly, the long-range hybrids do not improve the performance of these functionals significantly. The reoptimized functional oBLYP without the DFT-D correction is slightly better than the original BLYP but still underestimates the stabilities of the cyclophanes with a MAD of over 13 kcal/mol. Better performance is observed with the softer functionals (PBE family, M06-L, KT3, double hybrids with the PT2 term included) and for DFT-D corrected functionals, including Grimme’s B97-D and B2PLYP-D and oBLYP-D. The PBEsol functional is better than the original PBE (in agreement with previous reports by Csonka et al.⁶⁶). BPBE-D is again one of the best exchange-correlation combinations. MP2 overbinds compared to SOS-MP2.

A general conclusion can be reached that the stabilities of the cyclophanes are governed by the “normal” dispersion interactions that are dominated by correlation energy, with exchange being relatively unimportant. It was suggested⁷¹ that GGA exchange functionals have some contribution of the “left–right” correlation energy that is absent in the Hartree–Fock method; thus stand-alone exchange functionals perform slightly better than the Hartree–Fock method. The importance of the π – π correlation in cyclophanes was also previously noted by Grimme.³⁵ He termed the interactions “overlap-dispersion” and noted the poor performance of RHF as compared to SCS-MP2.

Let us consider the absolute values first for the polyhedranes **1a–4a**. The isomerization of **1a** to the dimethylnaphthalene **1e** is a highly exothermic process according to all of the methods we have used. Thus, while **1a** can be the most stable isomer of (CH)₁₂, it certainly is not the most stable C₁₂H₁₂ compound. Trends in the isomerization energy from **1a** to our reference **1b** are very similar to the tricyclododecatetraene **1d** that was used as the standard for the hydrogenated species **5a–c** and **7**; this confirms that both “standard” molecules are not pathological cases for DFT and/or MP2.

One important finding is that, similar to the hydrogenated **5a–c** and **7**, the polyhedranes with larger basal rings (**3a** and **4a**, which are free from the angular Bayer strain present in **1a** and **2a**) still show a similar picture of differences between the various density functionals: the BLYP, B86LYP, and GLYP combinations have larger errors than BPBE and OLYP; the DFT-D correction is insufficient to amend it. Interestingly, the optimized oBLYP functional, even with the DFT-D correction applied, has errors for polyhedrane stabilities that are smaller than the original BLYP but are

still significant, despite the fact that [D_{3d}]-octahedrane **1a** was included in its training set.⁶³

For the polyhedranes **1a–4a**, the isomerization energies are totally different from the ones for the cyclophanes, as was pointed out above already. By far, the largest differences with the SOS-MP2 isomerization energies, with a MAD of almost 70 kcal/mol, are given by the stand-alone B88 exchange, HFB. HFG fares only slightly better. The combinations of B88 exchange with the local correlation functionals, BW and BPW92, do not do well; the stand-alone OPTX-exchange HFO functional has a much smaller MAD of about 40 kcal/mol, comparable to the B86LYP, BLYP, GLYP, and BOP functionals. The latter functionals, along with oBLYP-D, perform worse than the RHF method (MAD of 22.1 kcal/mol). The double-hybrid B2PLYP functional and the B97-D functional have larger MADs than OLYP (15.3 kcal/mol). The TCA functional, which combines PBE exchange with a new Colle–Salvetti based GGA correlation functional, performs similarly (i.e., quite poorly) to the BLYP and GLYP functionals, despite the less repulsive character of the PBE exchange.

Using PBE correlation with OPTX exchange instead of LYP decreases the accuracy. The MADs for PBE and PBEsol are very close. However, the former systematically overestimates the reaction energies as compared to SOS-MP2, while the latter underestimates them (i.e., makes them more negative). Generally, application of the DFT-D correction for the “repulsive” functional reduces the MADs for the isomerization energies.

In contrast to the cyclophanes, for the polyhedranes, inclusion of the long-range HF corrections to the BLYP, GLYP, and BOP functionals dramatically improves their performance, to the extent that their results rank among those closest to the SOS-MP2 values. The OPTX-based double hybrid, in contrast to B2PLYP, performs very well also. Among the pure, uncorrected GGAs, the KT3 functional is the best, which makes it one of the few methods performing reasonably well for both the polyhedrane and cyclophane sets.

The popular global hybrid B3LYP, while more accurate than the pure BLYP functional, still has quite large errors for the cyclophanes and unacceptably large errors for the polyhedrane stabilities. For both series, it is outperformed by the newer power series B97 hybrid functional that includes a gradient corrected PW92 correlation part. It is interesting that the C-Pot modified B3LYP-C performs much better for the polyhedranes and especially well for the cyclophanes.

Summarizing the results for the polyhedrane series, we conclude that the higher MADs for some combinations, including the B88, B86, and G96 functionals, stem from large errors in the exchange functionals. Some of the GGA correlation functionals, such as the PBE correlation functional, can compensate the errors in the exchange, yielding successful combinations like BPBE; other functionals like LYP and OP do not yield this error compensation. The OLYP combination is better because the OPTX exchange has smaller errors than B88 and the like. The error seems to be related to the behavior of the DFT exchange in the long-range region, because application of range-separated hybrids

like BOP-LC where the long-range exchange is represented by the Hartree–Fock method fixes the problem.

Discussion

Previously, using relaxed PES scans for hydrocarbon collision (methane to neopentane), we²⁷ (as well as others, on similar systems⁶⁰) have shown that GGA functionals, uncorrected for the dispersion, are too repulsive; they can be arranged in the following way: OLYP > BLYP > B3LYP > BPBE > PBE > PBE1, MP2 > VWN5, in decreasing order of repulsiveness. Here, MP2 and VWN5 actually show overbinding. This statement requires a qualification; it was shown⁶⁰ that the character of the enhancement factor $F(x)$ of the exchange functional (eq 2) is responsible for the nonbonded interactions. For LDA exchange, $F(x)$ is constant; this leads to incorrect (different from the HF method) scaling and to spurious attraction at large interatomic distances, where the values of the reduced density gradient are high. Functionals that have $F(x)$ converging to a constant at large x show the same long-range overbinding; in order to get rid of it, $F(x)$ must have the “correct asymptotic behavior” (which, on the other hand, seems to contradict the Lieb–Oxford bound; see discussion in ref 72 and references therein). Of the functionals tested in our present work, G96 has the strongest dependence $F(x) \sim x^{3/2}$; then comes B88. The authors of ref 90 have shown that the optimal $F(x)$ scaling is $\sim x^{2/5}$, which held for the old P86⁹¹ GGA exchange functional. The rest of the exchange density functionals used in our work, including OLYP, are bound. However, at medium interatomic distances, the value and slope of $F(x)$ for intermediate values of x are important; here, the OLYP functional, which shows overbinding at large x , provides the strongest repulsion (which can be seen from Figures S1 and S2 of the Supporting Information). Since problems such as alkane intermolecular interactions fall into medium-range interatomic distances, one can say that OPTX is the most repulsive functional, followed by G96 and then B88. Let us now see how the repulsive character of these functionals affects the results for our model systems.

The dodecahedrane **3** has no small rings. However, it has angles around its carbon atoms of about 108.0°, which is lower than in free tertiary carbons—about 111° for isobutane. We have calculated deformation energies of the latter, optimizing its geometry with all CCC angles fixed to 108.0°. Results for selected GGA methods and MP2 are collected in Table S1 of the Supporting Information. The results show that the deformation energies for the isobutene are in line with the “repulsiveness” of the method—that is, they are highest for OLYP and lowest for VWN5 and MP2; the BLYP and B3LYP values are lower than those of OLYP. Therefore, the underestimation of the stability of dodecahedrane by BLYP and B3LYP cannot be ascribed to the angular deformation energies.

One can also observe that for polyhedranes **1a–4a**, due to their cage nature, all of the C–C dihedrals are in the eclipsed conformation. For that reason, a considerable sterical strain related to dihedral (1,4) interactions is present.^{4,38} Thus, to check whether the differences of the stabilities of these hydrocarbons are related to the description of the 1,4

interactions in saturated hydrocarbons, we have calculated the energy differences for *n*-butane in its *trans* and *cis* conformations (the latter being the rotational transition state). Results, again for the selected methods, are provided in Table S2 of the Supporting Information; they seem to show that for the 1,4 interactions, as well as for the 1,3 interactions described above, the order of the functionals follows their repulsiveness (OLYP > BLYP > PBE \gg VWN5), and the dispersion correction affects the results by stabilizing the *cis* conformer. Thus, the destabilization of the polyhedranes by BLYP as compared to OLYP probably cannot be explained by 1,4-nonbonded interactions similar to the ones in *n*-butane.

As was noted above, the enhancement factor $F(x)$ for the B86, B88, and G96 functionals differs at large values of x (see Figure S2, Supporting Information): while for B86, it converges to a limit, for G96, it diverges rapidly, and B88 shows intermediate behavior. But for small values of x , these exchange functionals are very similar to each other (and different from the OPTX functional). Since these functionals show very close results for the systems under study, the problems of polyhedrane stabilities can be ascribed to the small, not the large, values of the reduced density gradient. As the results show, the problems of the B86, B88, and G96 functionals with the description of polyhedranes can be fixed by matching them with the PBE correlation functional, but not with the LYP or OP ones.

An interesting question arising from this discussion is the following: why is the PBE correlation functional able to compensate for the B88 (B86, G96) errors, and why is this not happening for the LYP and OP functionals? The latter functionals are based on the Colle–Salvetti formula, while the former depends on the Perdew–Wang parametrization of the UEG correlation energy. Thus, various UEG limits are upheld by PBE but not by LYP. Both LYP and OP are also free from correlation self-interaction errors (i.e., yield zero correlation energy for a one-electron system), while PBE is not. Also, implicitly in LYP, and deliberately in the OP correlation functional, opposite-spin and same-spin correlation energies are treated differently—in the OP functional, in fact, the same-spin correlation term is not present; that is, it is said to be described by the matching exchange functional.

It was noticed in the literature⁹² that the Colle–Salvetti (CS) approach, while working well for atoms (however, see a recent study on the heavier atoms⁵³), underestimates “long-range” correlation that might be important for extended systems. UEG-parametrized correlation functionals such as PBE have a long-range correlation hole, which is said to be canceled by the exchange hole at long distances. The cancellation then does not happen if an exchange functional such as B88 is combined with a CS-based correlation counterpart.

It can be noted that reoptimization of the BLYP parameters, like the one done for the oBLYP-D functional, though resulting in some improvement, does not change the picture dramatically. Related functionals—the much simpler G96 and the earlier version, B86, that differs in its asymptotic behavior from B88—perform quite similarly. Interestingly, the original hybrid power series B97 functional performs much better

than B86LYP, BLYP, and B3LYP. The reason could again be that B97 has a correlation part that is based on UEG (PW92 functional,⁴⁴ with B97 gradient corrections, and different scaling of the same-spin and opposite-spin contributions).

Conclusions

The saturated cage molecules of the “polyhedrane” family $(CH)_n$, $n = 12, 16, 20, 24$ (**1a–4a**), were studied with a systematic variation of DFT exchange and correlation functionals and compared against the MP2 methods. The values computed with the SOS-MP2 method were used as the main reference. The stabilities of **1a–4a** were assessed by two methods: using the energies of formation from the acetylene $(CH)_2$ and by comparison with isomeric molecules chosen not to be problematic for DFT. For comparison, isomeric cyclophanes were considered, as systems with well-studied nonbonded intramolecular interaction patterns.

To our knowledge, polyhedranes $(CH)_{16}$ and $(CH)_{24}$ have not yet been synthesized, whereas $(CH)_{20}$ and $(CH)_{12}$ are known. Our computations predict that the stability of the former two molecules lies between those of the latter two. Thus, **2a** and **4a** could possibly be reasonable targets for synthesis.

The previously reported large discrepancies in the results of BLYP and B3LYP for **1a** cannot be explained by the angular strain or the presence of cyclopropane rings: our calculations have shown that hydrogenated derivatives of **1a** where the rings are opened show similar differences between the DFs; moreover, we have shown that dodecaedrane **3a**, which is free from the angular strain, exhibits the same problems with the B88 and LYP combination as does **1a**. In fact, throughout the entire polyhedrane set, the trend of the discrepancies of the DFT results compared to SOS-MP2 is similar.

The performance of density functional methods for the two sets, the polyhedranes and the cyclophanes, differs strongly. Methods that did well for one set often performed poorly for the other. For the cyclophanes, the correlation energy (long-range van der Waals dispersion and “overlap dispersion”, π – π correlation) is the determining factor of their stabilities: the more important, the closer the unsaturated rings get in the series **1c–4c**. For the polyhedranes, the errors in stability stem from the exchange functional, especially in the long-range region. A systematic study of stand-alone exchange functionals and their combinations with various correlation functionals shows that errors are much larger for the B88 and G96 functionals than for OPTX exchange. For the former two, the UEG-based PBE correlation functional somehow allows for error cancellation, while the Colle–Salvetti based LYP and OP correlation functionals fail to do that. Simple adjustment of the parameters of BLYP, as in the oBLYP-D functional, is insufficient to completely fix its performance. We propose that the difference is due to the ability of the UEG-based GGA correlation functionals to include long-range correlation effects that are absent in the Colle–Salvetti family of functionals.

For the polyhedranes, good results can be achieved by using long-range hybrids like BLYP-LC or BOP-LC. Among

the pure GGA functionals, the KT3 functional shows good performance on both sets of molecules.

Acknowledgment. This work is part of the Research Programme and was performed with financial support from the Dutch Polymer Institute (DPI), Eindhoven, The Netherlands, Project #641. We thank Dr. D. N. Laikov for providing us with the Priroda code. Part of the computations was performed at the high-performance computational facilities of the Canadian WestGrid consortium, which is funded in part by the Canada Foundation for Innovation, Alberta Innovation and Science, BC Advanced Education, and the participating research institutions.

Supporting Information Available: Details of basis sets used, MP2 optimized geometries of molecules **1–8**, and tables discussing isobutane deformation energies and *n*-butane rotational energies. This material is available free of charge via the Internet at <http://pubs.acs.org>.

References

- Schleyer, P. v. R.; Stang, P. J.; Raber, D. J. *J. Am. Chem. Soc.* **1970**, *92*, 4725.
- Paquette, L. A.; Balogh, D. W.; Usha, R.; Kountz, D.; Christoph, G. G. *Science* **1981**, *211*, 575.
- Paquette, L. A.; Ternansky, R. J.; Balogh, D. W.; Kentgen, G. *J. Am. Chem. Soc.* **1983**, *105*, 5446.
- Disch, R. L.; Schulman, J. M. *J. Phys. Chem.* **1996**, *100*, 3504.
- Wahl, F.; Weiler, A.; Landenberger, P.; Sackers, E.; Voss, T.; Haas, A.; Lieb, M.; Hunkler, D.; Worth, J.; Knothe, L.; Prinzbach, H. *Chem.—Eur. J.* **2006**, *12*, 6255.
- Karpushenkava, L. S.; Kabo, G. J.; Bazyleva, A. B. *THEOCHEM* **2009**, *913*, 43.
- de Meijere, A.; Lee, C. H.; Kuznetsov, M. A.; Gusev, D. V.; Kozhushkov, S. I.; Fokin, A. A.; Schreiner, P. R. *Chem.—Eur. J.* **2005**, *11*, 6175.
- Jia, J. F.; Liu, C.; Wu, H. S.; Schleyer, P. v. R.; Jiao, H. J. *J. Phys. Chem. C* **2009**, *113*, 8077.
- Cross, R. J.; Saunders, M.; Prinzbach, H. *Org. Lett.* **1999**, *1*, 1479.
- An, Y. P.; Yang, C. L.; Wang, M. S.; Ma, X. G.; Wang, D. H. *J. Phys. Chem. C* **2009**, *113*, 15756.
- Gapurenko, O. A.; Gribanova, T. N.; Minyaev, R. M.; Minkin, V. I. *Russ. Chem. Bull.* **2007**, *56*, 856.
- Johnson, E. R.; Mori-Sanchez, P.; Cohen, A. J.; Yang, W. T. *J. Chem. Phys.* **2008**, *129*, 204112.
- Schreiner, P. R. *Angew. Chem., Int. Ed.* **2007**, *46*, 4217.
- Schreiner, P. R.; Fokin, A. A.; Pascal, R. A.; de Meijere, A. *Org. Lett.* **2006**, *8*, 3635.
- Wodrich, M. D.; Corminboeuf, C.; Schreiner, P. R.; Fokin, A. A.; Schleyer, P. v. R. *Org. Lett.* **2007**, *9*, 1851.
- Grimme, S. *Angew. Chem., Int. Ed.* **2006**, *45*, 4460.
- Grimme, S.; Steinmetz, M.; Korth, M. *J. Chem. Theory Comput.* **2007**, *3*, 42.
- Brittain, D. R. B.; Lin, C. Y.; Gilbert, A. T. B.; Izgorodina, E. I.; Gill, P. M. W.; Coote, M. L. *Phys. Chem. Chem. Phys.* **2009**, *11*, 1138.
- Izgorodina, E. I.; Coote, M. L.; Radom, L. *J. Phys. Chem. A* **2005**, *109*, 7558.
- Johnson, E. R.; Mackie, I. D.; DiLabio, G. A. *J. Phys. Org. Chem.* **2009**, *22*, 1127.
- Schwabe, T.; Grimme, S. *Acc. Chem. Res.* **2008**, *41*, 569.
- Grimme, S. *J. Comput. Chem.* **2004**, *25*, 1463.
- Grimme, S. *J. Comput. Chem.* **2006**, *27*, 1787.
- von Lilienfeld, O. A.; Tavernelli, I.; Rothlisberger, U.; Sebastiani, D. *Phys. Rev. Lett.* **2004**, *93*, 4.
- Mackie, I. D.; DiLabio, G. A. *J. Phys. Chem. A* **2008**, *112*, 10968.
- Mackie, I. D.; McClure, S. A.; DiLabio, G. A. *J. Phys. Chem. A* **2009**, *113*, 5476.
- Shamov, G. A.; Budzelaar, P. H. M.; Schreckenbach, G. *J. Chem. Theory Comput.* **2010**, *6*, 477.
- Wodrich, M. D.; Jana, D. F.; Schleyer, P. V. R.; Corminboeuf, C. *J. Phys. Chem. A* **2008**, *112*, 11495.
- Grimme, S.; Antony, J.; Ehrlich, S.; Krieg, H. *J. Chem. Phys.* **2010**, *132*.
- Becke, A. D. *Phys. Rev. A* **1988**, *38*, 3098.
- Lee, C. T.; Yang, W. T.; Parr, R. G. *Phys. Rev. B* **1988**, *37*, 785.
- Miehlich, B.; Savin, A.; Stoll, H.; Preuss, H. *Chem. Phys. Lett.* **1989**, *157*, 200.
- Gill, P. M. W. *Mol. Phys.* **1996**, *89*, 433.
- Caramori, G. F.; Galembeck, S. E. *J. Phys. Chem. A* **2008**, *112*, 11784.
- Grimme, S. *Chem.—Eur. J.* **2004**, *10*, 3423.
- Kamya, P. R. N.; Muchall, H. M. *J. Phys. Chem. A* **2008**, *112*, 13691.
- Schleyer, P. v. R.; Williams, J. E.; Blanchard, K. R. *J. Am. Chem. Soc.* **1970**, *92*, 2377.
- Beckhaus, H. D.; Ruchardt, C.; Lagerwall, D. R.; Paquette, L. A.; Wahl, F.; Prinzbach, H. *J. Am. Chem. Soc.* **1994**, *116*, 11775.
- Grimme, S.; Steinmetz, M.; Korth, M. *J. Org. Chem.* **2007**, *72*, 2118.
- Ikura, H.; Tsuneda, T.; Yanai, T.; Hirao, K. *J. Chem. Phys.* **2001**, *115*, 3540.
- Song, J. W.; Hirose, T.; Tsuneda, T.; Hirao, K. *J. Chem. Phys.* **2007**, *126*, 7.
- Grimme, S. *J. Chem. Phys.* **2006**, *124*, 034108.
- Vosko, S. H.; Wilk, L.; Nusair, M. *Can. J. Phys.* **1980**, *58*, 1200.
- Perdew, J. P.; Wang, Y. *Phys. Rev. B* **1992**, *45*, 13244.
- Proynov, E.; Kong, J. *Phys. Rev. A* **2009**, *79*, 4.
- Van Voorhis, T.; Scuseria, G. E. *J. Chem. Phys.* **1998**, *109*, 400.
- Zhao, Y.; Truhlar, D. G. *Theor. Chem. Acc.* **2008**, *120*, 215.
- Stewart, P. A.; Gill, P. M. W. *J. Chem. Soc., Faraday Trans.* **1995**, *91*, 4337.
- Tsuneda, T.; Suzumura, T.; Hirao, K. *J. Chem. Phys.* **1999**, *110*, 10664.
- Handy, N. C.; Cohen, A. J. *J. Chem. Phys.* **2002**, *116*, 5411.

- (51) Ragot, S.; Cortona, P. *J. Chem. Phys.* **2004**, *121*, 7671.
- (52) Tognetti, V.; Cortona, P.; Adamo, C. *J. Chem. Phys.* **2008**, *128*, 034101.
- (53) Thakkar, A. J.; McCarthy, S. P. *J. Chem. Phys.* **2009**, *131*, 12.
- (54) Becke, A. D. *J. Chem. Phys.* **1993**, *98*, 5648.
- (55) Krukau, A. V.; Scuseria, G. E.; Perdew, J. P.; Savin, A. *J. Chem. Phys.* **2008**, *129*, 7.
- (56) Janesko, B. G.; Henderson, T. M.; Scuseria, G. E. *J. Chem. Phys.* **2009**, *131*, 9.
- (57) Weintraub, E.; Henderson, T. M.; Scuseria, G. E. *J. Chem. Theory Comput.* **2009**, *5*, 754.
- (58) Peach, M. J. G.; Helgaker, T.; Salek, P.; Keal, T. W.; Lutnaes, O. B.; Tozer, D. J.; Handy, N. C. *Phys. Chem. Chem. Phys.* **2006**, *8*, 558.
- (59) Becke, A. D.; Johnson, E. R. *J. Chem. Phys.* **2007**, 127.
- (60) Zhang, Y. K.; Pan, W.; Yang, W. T. *J. Chem. Phys.* **1997**, *107*, 7921.
- (61) Swart, M.; van der Wijst, T.; Guerra, C. F.; Bickelhaupt, F. M. *J. Mol. Model.* **2007**, *13*, 1245.
- (62) Becke, A. D. *J. Chem. Phys.* **1997**, *107*, 8554.
- (63) Goerigk, L.; Grimme, S. *J. Chem. Theory Comput.* **2010**, *6*, 107.
- (64) Keal, T. W.; Tozer, D. J. *J. Chem. Phys.* **2004**, *121*, 5654.
- (65) Perdew, J. P.; Ruzsinszky, A.; Csonka, G. I.; Vydrov, O. A.; Scuseria, G. E.; Constantin, L. A.; Zhou, X. L.; Burke, K. *Phys. Rev. Lett.* **2008**, 100.
- (66) Csonka, G. I.; Ruzsinszky, A.; Perdew, J. P.; Grimme, S. *J. Chem. Theory Comput.* **2008**, *4*, 888.
- (67) Ruzsinszky, A.; Csonka, G. I.; Scuseria, G. E. *J. Chem. Theory Comput.* **2009**, *5*, 763.
- (68) Colle, R.; Salvetti, O. *Theor. Chim. Acta* **1975**, *37*, 329.
- (69) Tognetti, V.; Cortona, P.; Adamo, C. *Chem. Phys. Lett.* **2007**, *439*, 381.
- (70) Handy, N. C. *Theor. Chem. Acc.* **2009**, *123*, 165.
- (71) Handy, N. C.; Cohen, A. J. *Mol. Phys.* **2001**, *99*, 403.
- (72) Perdew, J. P.; Burke, K.; Ernzerhof, M. *Phys. Rev. Lett.* **1996**, *77*, 3865.
- (73) Laikov, D. N. *Chem. Phys. Lett.* **1997**, *281*, 151.
- (74) Laikov, D. N. *Chem. Phys. Lett.* **2005**, *416*, 116.
- (75) Laikov, D. N.; Ustynyuk, Y. A. *Russ. Chem. Bull.* **2005**, *54*, 820.
- (76) Aquilante, F.; De Vico, L.; Ferre, N.; Ghigo, G.; Malmqvist, P. A.; Neogrady, P.; Pedersen, T. B.; Pitonak, M.; Reiher, M.; Roos, B. O.; Serrano-Andres, L.; Urban, M.; Veryazov, V.; Lindh, R. *J. Comput. Chem.* **2010**, *31*, 224.
- (77) Karlstrom, G.; Lindh, R.; Malmqvist, P. A.; Roos, B. O.; Ryde, U.; Veryazov, V.; Widmark, P. O.; Cossi, M.; Schimmelpfennig, B.; Neogrady, P.; Seijo, L. *Comput. Mater. Sci.* **2003**, *28*, 222.
- (78) Wigner, E. *Trans. Faraday Soc.* **1938**, *34*, 678.
- (79) Molawi, K.; Cohen, A. J.; Handy, N. C. *Int. J. Quantum Chem.* **2002**, *89*, 86.
- (80) Jung, Y. S.; Lochan, R. C.; Dutoi, A. D.; Head-Gordon, M. *J. Chem. Phys.* **2004**, *121*, 9793.
- (81) Pedersen, T. B.; Aquilante, F.; Lindh, R. *Theor. Chem. Acc.* **2009**, *124*, 1.
- (82) Bostrom, J.; Aquilante, F.; Pedersen, T. B.; Lindh, R. *J. Chem. Theory Comput.* **2009**, *5*, 1545.
- (83) Aquilante, F.; Gagliardi, L.; Pedersen, T. B.; Lindh, R. *J. Chem. Phys.* **2009**, 130.
- (84) Pitonak, M.; Neogrady, P.; Cerny, J.; Grimme, S.; Hobza, P. *ChemPhysChem* **2009**, *10*, 282.
- (85) Budzelaar, P. H. M. *J. Comput. Chem.* **2007**, *28*, 2226.
- (86) Gordon, M. S.; Schmidt, M. W. *In Theory and Applications of Computational Chemistry: the First Forty Years*; Dykstra, C. E., Frenking, G., Kim, K. S., Scuseria, G. E., Eds.; Elsevier: Amsterdam, 2005; p 1167.
- (87) Dunning, T. H.; Hay, P. J. *In Methods of Electronic Structure Theory*; Schaefer, H. F., Ed.; Plenum Press: New York, 1977; p 1.
- (88) Steinmann, S. N.; Csonka, G.; Corminboeuf, C. *J. Chem. Theory Comput.* **2009**, *5*, 2950.
- (89) Grimme, S. *Angew. Chem., Int. Ed.* **2008**, *47*, 3430.
- (90) Murray, E. D.; Lee, K.; Langreth, D. C. *J. Chem. Theory Comput.* **2009**, *5*, 2754.
- (91) Perdew, J. P. *Phys. Rev. B* **1986**, *33*, 8822.
- (92) Tao, J. M.; Gori-Giorgi, P.; Perdew, J. P.; McWeeny, R. *Phys. Rev. A* **2001**, *63*, 032513.

CT100389D